PAPER

Optimizing volumetric surface area of UiO-66 and its functionalized analogs through compression†

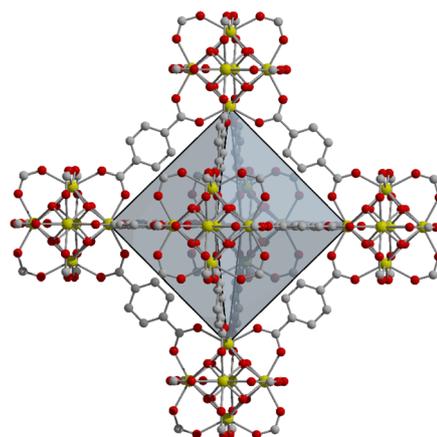Andrew Kuznicki[a] and Eric D. Bloch [iD] *[ab]

Metal–organic frameworks (MOFs) have garnered significant attention as gas storage materials due to their exceptional surface areas and customizable pore chemistry. For applications in the storage of small molecules for vehicular transportation, achieving high volumetric capacities is crucial. In this study, we demonstrate the compression of UiO-66 and a series of its functionalized analogs at elevated pressures, resulting in the formation of robust pellets with significantly increased volumetric surface areas. The optimal compression pressure is found to be contingent on the specific nature of the functional group attached to the organic linker in the MOF material.

Over the past 25 years, metal–organic frameworks (MOFs) have undergone extensive investigation for a wide range of applications.[1] These studies have encompassed areas including gas storage, separations, catalysis, and sensing, leading to diverse and targeted research.[2] Demonstrating the potential impact of these materials, recent efforts have shifted towards practical considerations. For instance, researchers have moved from merely exploring new reactivity profiles to conducting cycling and poisoning studies for MOF catalysts.[3] In the context of gas storage, current research has focused on scaling up materials beyond lab-scale solvothermal reactions.[4] Moreover, for real-world storage applications, emphasis has shifted towards the usability of promising MOFs.[5] In contrast to fundamental academic studies, large-scale implementation of adsorbent materials requires processable forms, such as pellets,[6] extrudates,[7] or monoliths.[8] These efforts reflect a growing interest in the practical applicability of MOFs and their potential impact on various industries.

Monoliths or extrudates are highly appealing since the synthesis of materials and their subsequent processing into shapes are typically accomplished within the same synthesis steps.[9] Solvothermal syntheses may afford dense monoliths and solvent-free mechanochemistry may afford high-surface area pellets.[10,11] The former, however, is not translatable to all materials while the latter often affords non-ideal materials with lower surface areas and/or crystallinities.[12] Post-synthetic compression may offer advantages here as low-density bulk powders can be transformed into dense, processable pellets *via*

the application of mechanical force.[13,14] In terms of gas storage applications, this densification is important for realizing higher volumetric storage capacities.[15] In reality, most gas storage capacities reported for MOFs are based on crystallographic densities although the actual bulk densities of samples are only a fraction of them.[16]

Unfortunately, many MOFs are not compatible with compression and/or pelletization as the metal–ligand bonds that comprise these hybrid materials break down at moderate pressures.[17] Beyond this, systematic studies correlating structural factors with MOF stability are lacking. The work reported here is aimed at broadening the understanding of optimal compression for a functionalized family of MOFs, UiO-66 (Fig. 1). We ultimately investigate the effects of ligand

[a]Department of Chemistry and Biochemistry, University of Delaware, Newark, Delaware 19716, USA

[b]Department of Chemistry, Indiana University, Bloomington, Indiana 47405, USA. E-mail: edbloch@iu.edu

† Electronic supplementary information (ESI) available. See DOI: https://doi.org/10.1039/d3ra03668e

Fig. 1 A portion of the structure of UiO-66 where yellow, red, and gray spheres represent zirconium, oxygen, and carbon atoms, respectively. Hydrogen atoms have been omitted for clarity. UiO-66-NH_2 features disordered 2-position functionalization of terephthalic acid with $-NH_2$. These groups have also been omitted.

functionalization on maximum volumetric surface area for a series of amide-functionalized MOFs.

Unfunctionalized UiO-66 was targeted as the starting point for this work given its moderate surface area and its well know thermal,[18] chemical,[19] and hydrolytic stabilities.[20] Although defect-free material has a Langmuir surface area just over 1000 $m^2 g^{-1}$, when using mineral or organic acids to modulate the particle size of the material, ligand or cluster-defective samples can be isolated;[21] these specific materials have significantly increased gravimetric surface areas. Indeed an HCl modulated synthesis affords a sample, upon appropriate solvent exchange and activation, with a Langmuir surface area of 1385 $m^2 g^{-1}$, as determined using nitrogen adsorption at 77 K. Given the low bulk density of this free-flowing powder, it has a volumetric surface area of just 320 $m^2 mL^{-1}$. We expected mechanical compression of the sample to afford significantly increased volumetric surface areas. Indeed, compression of an activated powder to just 0.15 GPa affords material with a volumetric surface area of 622 $m^2 g^{-1}$, nearly double the free powder. Although mechanical compression and pelletization does serve to densify the material, it does so at the expense of gravimetric surface area, which slightly decreases at this pressure to 1171 $m^2 g^{-1}$. In order to determine the optimal compression pressure, we further prepared pellets by compressing different powder samples to 0.40, 0.65, and 1.01 GPa. At pressures above 0.40 GPa, we observe significant losses in gravimetric surface area. This is in contrast to previous reports of UiO-66 pelletization where it was found that at compression pressures up to 0.665 GPa afforded a material with only slightly diminished BET surface area as compared to the bulk powder (1707 vs. 1737 $m^2 g^{-1}$),[22] although the previous report utilized a different pelletization geometry and starting surface area, and thus defect level, sample. The surface area decrease we observed is in line with those previously reported for UiO-66-NH$_2$ where pelletization pressures of 0.127 or 0.164 GPa resulted in surface area losses of 26%.[23,24] It is important to note that the losses in gravimetric surface area are offset by increasing density and samples with gravimetric surface areas under 500 $m^2 g^{-1}$ display volumetric surface areas in excess of 675 $m^2 mL^{-1}$ (Table 1). We found an optimal compression pressure of 0.40 GPa afforded a material with a gravimetric surface area of 1278 $m^2 g^{-1}$ and a volumetric surface area of 965 $m^2 g^{-1}$, more than 3× greater than the starting value.

In order to attenuate some of the deleterious effects of compression on UiO-66 samples, we turned to functionalized ligands, as these have previously been shown to be a viable handle for tuning the properties of many MOFs,[25] UiO-66 in particular. A number of functionalized UiO-66 analogs have been reported, and the attached functional groups have included aryl, alkyl, and halide substituents, among others.[26,27] To more systematically probe the effects of ligand functionalization, we turned to amide functionalization as it is a straightforward route to attaching increment length to the ligand side chains.[28] Here, the reaction of 2-aminoterephthalic acid with acyl chlorides affords amide-functionalized ligands in nearly quantitative yield. For the work performed here we utilized acetyl, 3,5,5-hexanoyl, and lauroyl chloride to give ligands with 2, 6, and 12 carbon atoms, respectively, on their side chains. With the addition of 2-amino terephthalic acid, this gave us four additional ligands to survey in this compression study (Fig. 2). Similar to the synthesis of UiO-66, reaction of ZrCl$_4$ with organic linker in DMF at elevated temperature affords functionalized MOF in nearly quantitative yield. Here too, addition of acid to the synthesis increases particle size with minimal changes in crystallinity. Surface area analyses on activated samples result in the expected trends with increased ligand bulk affording material with decreases surface area. The MOFs display BET surface areas ranging from 700–1600 $m^2 g^{-1}$ that follow the trend NH$_2$ > acetyl > hexanoyl > lauroyl. Volumetric surface areas follow a similar trend with the acetyl giving the lowest surface area framework. It is of note that functionalized MOFs have a smaller range of volumetric surface areas with measured values from 225–525 $m^2 mL^{-1}$.

Similar to parent UiO-66, all four samples displayed varying levels of compatibility with compression (Fig. 3). UiO-66-NH$_2$ had a gradual drop in gravimetric surface area with increasing pressures where its Langmuir surface area dropped from ∼1600 $m^2 g^{-1}$ to 450 $m^2 g^{-1}$ at just over 1 GPa of compression. This material had a maximum volumetric surface area of 825 $m^2 mL^{-1}$ at a compression pressure of 0.40 GPa. As a result of the relatively high density of the material, compression only served to increase volumetric surface area by ∼300 $m^2 mL^{-1}$. Compression proved valuable for both UiO-66-acetyl and UiO-66-hexanoyl as their pelletized samples have higher surface
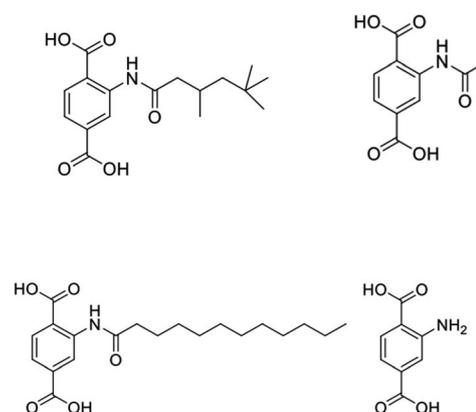

Fig. 2 Functionalized terephthalic acid ligands used in this study where acetal (top right), hexanoyl (top left) and lauroyl (bottom left) are appended on 2-aminotherephtahlc acid (bottom right) via straightforward acylation chemistry.

Table 1 Compression and surface area data for UiO-66

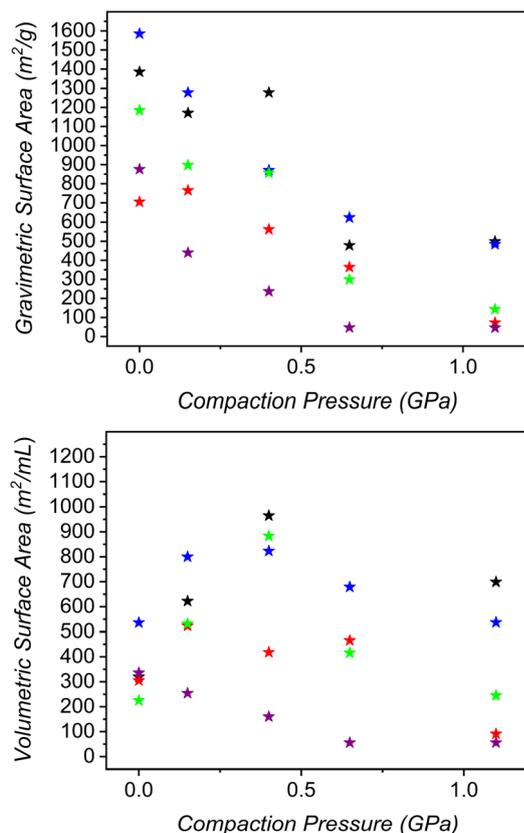| GPa	PSIG	Mg	Gravimetric SA ($m^2 g^{-1}$)	Density (g mL^{-1})	Volumetric SA ($m^2 mL^{-1}$)
0	0	0	1385	0.23	320
0.15	21 732	0.3	1171	0.53	622
0.40	57 952	0.8	1278	0.76	965
0.65	94 171	1.3	478	1.42	679
1.01	159 367	2.2	499	1.40	699

Fig. 3 Gravimetric (top) and volumetric (bottom) for UiO-66 (black) as compared to $-NH_2$ (blue), acetyl (green), 3,5,5-trimethylhexanoyl (red), and lauroyl-amide (purple) functionalized framework.

areas than pure powder. Similar to UiO-66 and UiO-66-NH_2, the acetyl functionalized material has a maximum volumetric surface area after compression with 0.40 GPa. The hexanoyl material, however, has an optimized volumetric surface area after compression to just 0.15 GPa. The acetyl-functionalized MOF shows a marked decrease in volumetric surface area when compressed to higher pressures while the hexanoyl MOF actually displays a modest drop at 0.40 GPa and an increase at 0.65 GPa before becoming nonporous after compression at 1 GPa. The volumetric surface area of the lauroyl-functionalized MOF was not increased with compression. This material displayed the highest surface area as a powder and became completely nonporous to N_2 at a compression pressure of just 0.65 GPa. This is not entirely unexpected as the bulky functional groups on the ligand occupy significant pore space and render the pores inaccessible at even modest compression pressures. We generally found that higher compression pressures afforded more robust pellets.

The gravimetric and volumetric surface areas of samples under equilibrium conditions are important considerations for the performance of adsorptive materials. However, adsorption kinetics and cyclability are also important, particularly if MOFs are to be employed on an industrial setting. The inherently increased cost of the materials require longer lifetimes and/or rapid adsorption/desorption kinetics. In order to more fully

quantify these, we utilized thermogravimetric analysis where an activated sample of powder or pellet was heated under an N_2 flow to elevated temperature to fully desolvate the MOF. We then cooled the samples to subject them to CO_2/N_2 cycling experiments. This facile and rapid test can interrogate both adsorption kinetics and provides some information about cyclability. As expected, the pelletized sample of UiO-66 has lower gravimetric CO_2 uptake, there are no notable differences in adsorption kinetics or desorption kinetics (Fig. S8†) which is expected given the relatively high retention of surface area. Importantly, the pelletized sample also shows no loss in adsorption capacity after over 100 cycles. Visual inspection of the sample after the cycling experiment reveals it maintains its pelletized form, confirming the sample is also mechanically robust upon cycling.

The foregoing results demonstrate the importance of ligand functionalization on the compressibility of a specific family of MOFs (UiO-66). Although the unfunctionalized MOF had the highest volumetric surface area, a result of its high gravimetric surface area, ligand functionalization imparts additional mechanical stability to a subset of samples at higher compression pressures. There is also an important correlation between mechanical stability and compression pressure where denser samples have higher stability. Our work here suggests that although functional groups decrease both volumetric and gravimetric surface areas, their presence can be leveraged to maximize mechanical stability while modulating surface areas losses.

Conflicts of interest

There are no conflicts to declare.

References

1 R. Freud, S. Canossa, S. M. Cohen, W. Yan, H. Deng, V. Guilerm, M. Eddaoudi, D. G. Madden, D. Fairen-Jimenez, H. Lyu, L. K. Macreadie, Z. Ji, Y. Zhang, B. Wang, F. Haase, C. Woll, O. Zaremba, J. Andreo, S. Wuttke and C. S. Diercks, *Angew. Chem., Int. Ed.*, 2021, **60**, 23946–23974.

2 W. Fan, X. Wang, B. Xu, Y. Wang, D. Liu, M. Zhang, Y. Shang, F. Dai, L. Zhang and D. Sun, *J. Mater. Chem. A*, 2018, **6**, 24486–24495.

3 S. Bao, J. Li, B. Guan, M. Jiak, O. Terasaki and J. Yu, *Matter*, 2020, **3**, 332–334.

4 Y. Zhao, Q. Zhang, Y. Li, R. Zhang and G. Lu, *ACS Appl. Mater. Interfaces*, 2017, **9**, 15079–15085.

5 B. M. Connolly, D. G. Madden, A. E. H. Wheatley and D. Fairen-Jimenez, *J. Am. Chem. Soc.*, 2020, **142**(19), 8541–8549.

6 B. Yeskendir, J.-P. Dacquin, Y. Lorgouilloux, C. Courtois, S. Royer and J. Dhainaut, *Adv. Mater.*, 2021, **2**, 7139–7186.

7 S. Pu, J. Wang, L. Li, Z. Zhang, Z. Bao, Q. Yang, Y. Yang, H. Xing and Q. Ren, *Ind. Eng. Chem. Res.*, 2018, **57**, 1645–1654.

8 B. Yeskendir, J. Dacquin, Y. Longouilloux, C. Courtois, S. Royer and J. Dhainaut, *Adv. Mater.*, 2021, **2**, 7139–7186.

9 V. Ntouros, I. Kousis, A. L. Pisello and M. N. Assimakopoulos, *Energies*, 2022, **15**, 1489.

10 J. Bemish-Cook, K. Shankland, C. A. Murray and P. Vaqueiro, *Cryst. Growth Des.*, 2021, **21**, 3047–3055.

11 E. Tsalaporta and J. M. D. MacElroy, *Heliyon*, 2020, **6**, 4883.

12 R. Sule and A. K. Mishra, *Appl. Sci.*, 2019, **9**, 4407.

13 S. E. Bambalaza, H. W. Langmi, R. Mokaya, N. M. Musyoka and O. E. Khotseng, *ACS Appl. Mater. Interfaces*, 2020, **12**, 24883–24894.

14 G. W. Peterson, J. B. DeCost, T. G. Glover, Y. Huang, H. Jasuja and K. S. Walton, *Microporous Mesoporous Mater.*, 2013, **179**, 48–53.

15 B. M. Connolly, M. Aragones-Anglada, D. N. A. Gandara-Loe, D. Lamb, J. P. Mehta, D. Vulpe, S. Wuttke, J. Silvestre-Albero, P. Z. Moghadam, A. E. H. Wheatley and D. Fairen-Jimenez, *Nat. Commun.*, 2019, **10**, 2345.

16 K. Suresh, D. Aulakh, J. Purewal, D. J. Siegel, M. Beenstra and A. J. Matzger, *J. Am. Chem. Soc.*, 2021, **143**, 10727–10734.

17 S. Yuan, X. Sun, J. Pang, C. Lollar, J. S. Qin, Z. Perry and H. C. Zhou, *Joule*, 2017, **1**, 806–815.

18 M. Athat, P. Rzepka, D. Thoeny, M. Ranocchiari and J. A. von Bokhoven, *RSC Adv.*, 2021, **11**, 38849–38855.

19 D. Buzek, S. Adamec, K. Lang and J. Demel, *Inorg. Chem. Front.*, 2021, **8**, 720–734.

20 D. Buzek, J. Demel and K. Lang, *Inorg. Chem.*, 2018, **57**, 14290–14297.

21 X. Chen, Y. Li, Q. Fu, H. Qin, J. Lv, K. Yang, Q. Zhang, H. Zhang and M. Wang, *RSC Adv.*, 2022, **12**, 6083–6092.

22 S. E. Bambalaza, H. W. Langmi, R. Mokaya, N. M. Musyoka, J. Ren and L. E. Khotseng, *J. Mater. Chem. A*, 2018, **6**, 23569–23577.

23 J. Dhainaut, J. Troyano, A. Legrand, J. Canivet, I. Imaz, D. Maspoch, H. Reinsch and D. Farrusseng, *CrystEngComm*, 2017, **19**, 4211–4218.

24 G. W. Peterson, J. B. Decoste, F. Fatollahi-fard and D. K. Britt, *Ind. Eng. Chem. Res.*, 2014, **53**, 701–707.

25 P. Deria, W. Bury, I. Hod, C.-W. Kung, O. Karagiaridi, J. T. Hupp and O. K. Farha, *Inorg. Chem.*, 2015, **54**, 2185–2192.

26 Y. Khabzina, J. Dhainaut, M. Anlhelm, H.-J. Richter, H. Reinsch, N. Stock and D. Farrusseng, *Ind. Eng. Chem. Res.*, 2018, **57**, 8200–8208.

27 R. D'Amato, R. Bondi, I. Moghdad, F. Marmottini, M. J. McPherson, H. Naili, M. Taddei and F. Contantino, *Inorg. Chem.*, 2021, **60**, 14294–14301.

28 A. Kuznicki, G. R. Lorzing and E. D. Bloch, *Chem. Commun.*, 2021, **57**, 8312–8315.